



# DT-13 Ameliorates TNF- $\alpha$ -Induced Vascular Endothelial Hyperpermeability via Non-Muscle Myosin IIA and the Src/PI3K/Akt Signaling Pathway

Yuanyuan Zhang, Yuwei Han, Yazheng Zhao, Yanni Lv, Yang Hu, Yisha Tan, Xueyuan Bi, Boyang Yu\* and Junping Kou\*

State Key Laboratory of Natural Products, Jiangsu Key Laboratory of TCM Evaluation and Translational Research, Department of Complex Prescription of TCM, China Pharmaceutical University, Nanjing, China

## OPEN ACCESS

### Edited by:

Annalisa Bruno,  
Università degli Studi  
"G. d'Annunzio" Chieti-Pescara, Italy

### Reviewed by:

Annalisa Trenti,  
University of Padua, Italy  
Aitor Aguirre,  
University of California, San Diego,  
United States

### \*Correspondence:

Boyang Yu  
boyangyu59@163.com;  
Junping Kou  
junpingkou@cpu.edu.cn

### Specialty section:

This article was submitted to  
Inflammation Pharmacology,  
a section of the journal  
Frontiers in Immunology

Received: 24 March 2017

Accepted: 20 July 2017

Published: 14 August 2017

### Citation:

Zhang Y, Han Y, Zhao Y, Lv Y, Hu Y,  
Tan Y, Bi X, Yu B and Kou J (2017)  
DT-13 Ameliorates TNF- $\alpha$ -Induced  
Vascular Endothelial  
Hyperpermeability via Non-Muscle  
Myosin IIA and the Src/PI3K/Akt  
Signaling Pathway.  
Front. Immunol. 8:925.  
doi: 10.3389/fimmu.2017.00925

DT-13(25(R,S)-ruscogenin-1-O-[ $\beta$ -D-glucopyranosyl-(1 $\rightarrow$ 2)] [ $\beta$ -D-xylopyranosyl-(1 $\rightarrow$ 3)]- $\beta$ -D-fucopyranoside) has been identified as an important factor in TNF- $\alpha$ -induced vascular inflammation. However, the effect of DT-13 on TNF- $\alpha$ -induced endothelial permeability and the potential molecular mechanisms remain unclear. Hence, this study was undertaken to elucidate the protective effect of DT-13 on TNF- $\alpha$ -induced endothelial permeability and the underlying mechanisms *in vivo* and *in vitro*. The *in vivo* results showed that DT-13 could ameliorate endothelial permeability in mustard oil-induced plasma leakage in the skin and modulate ZO-1 organization. In addition, the *in vitro* results showed that pretreatment with DT-13 could increase the transendothelial electrical resistance value and decrease the sodium fluorescein permeability coefficient. Moreover, DT-13 altered the mRNA and protein levels of ZO-1 as determined by real-time PCR, Western blotting, and immunofluorescence analyses. DT-13 treatment decreased the phosphorylations of Src, PI3K, and Akt in TNF- $\alpha$ -treated human umbilical vein endothelial cells (HUVECs). Further analyses with PP2 (10  $\mu$ M, inhibitor of Src) indicated that DT-13 modulated endothelial permeability in TNF- $\alpha$ -induced HUVECs in a Src-dependent manner. LY294002 (10  $\mu$ M, PI3K inhibitor) also had the same effect on DT-13 but did not affect phosphorylation of Src. Following decreased expression of non-muscle myosin IIA (NMIIA), the effect of DT-13 on the phosphorylations of Src, PI3K, and Akt was abolished. This study provides pharmacological evidence showing that DT-13 significantly ameliorated the TNF- $\alpha$ -induced vascular endothelial hyperpermeability through modulation of the Src/PI3K/Akt pathway and NMIIA, which play an important role in this process.

**Keywords:** DT-13, vascular endothelial hyperpermeability, tight junctions, Src/PI3K/Akt, non-muscle myosin IIA

## INTRODUCTION

Alterations in endothelial barrier function play an important role in the pathogenesis of many disease conditions, including immunology diseases, sepsis, inflammation, wound healing, edema, acute lung injury (ALI), stroke, and cancer (1–3). The integrity of the vascular endothelial cell layer is maintained by intercellular complexes composed of tight junctions (TJs), adherens junctions,

and gap junctions (4). TJs, the most luminal component of the apical junctional complex, form a barrier that limits paracellular movement of water, ions, and macromolecules (5). Recently, TNF- $\alpha$ -induced barrier dysfunction has been shown to be a critical contributor to human disease. TNF- $\alpha$ -induced inflammatory changes to endothelial cells include protein synthesis-independent changes in cell permeability and cell motility, leading to localized inflammatory responses, vascular leakage, and edema formation. TNF- $\alpha$ -induced permeability underlies the pathobiology of several disorders (6, 7). Therefore, it is important to investigate the ability of drugs used to treat various diseases to protect endothelial cell permeability.

Different proteins have been shown to be located in TJs, including ZO-1, ZO-2, ZO-3, occludin, and claudins (8). TJs prevent diffusion of molecules between adjacent endothelial cells and maintain endothelial tightness. ZO-1 was the first TJ protein described, and it is critical for junction assembly and permeability. In the absence of ZO-1, cells fail to form TJs (9, 10). The ZO-1 protein not only combines with cytoplasmic and transmembrane proteins but also interacts with ZO-2 or ZO-3 to form a complex in the cell that principally acts as a bridge. The cell membrane protein occludin and the intracellular skeleton component actin interact to form a stable structural system, and the other proteins are closely involved in this structure (11, 12). In many cases, ZO-1 dysfunction or distribution changes destroy the integrity of the TJs between cells, causing gap increases, which result in increased vascular permeability. Thus, ZO-1 has been used as a marker of barrier integrity and permeability (13). ZO-1 knockout in Eph4 cells resulted in TJ damage (9).

Src family kinases are a class of non-receptor tyrosine kinases involved in the modulation of cell survival, proliferation, differentiation, and migration. In some cells, Src is a critical upstream regulator of steroid-stimulated membrane signal transduction pathways (14). Knockdown (KD) of Src accelerates oxidative stress-induced assembly of TJs and restoration of the barrier function (15). In addition, Src promotes PI3K *via* the Src association with the p85 subunit of PI3K (16). The class I PI3K and the serine/threonine-specific protein kinase Akt signaling pathway (PI3K/AKT) is one of the most important pathways involved in inflammatory responses (17). The increase in endothelial permeability and ZO-1 alteration induced by pro-inflammatory cytokines may be related to the PI3K/Akt pathway (18).

Non-muscle myosin II consists of a group of molecular motors, including three paralogs (IIA, IIB, and IIC), which are involved in a wide variety of cellular processes, including cytokinesis, proliferation, adhesion, migration, and control of cell morphology (19–21). Non-muscle myosin IIA (NMIIA) plays an important role in inflammation and could be a target for inflammatory disease therapy (22). In inflammatory bowel disease patients, steady-state levels of atypical PKC in the active conformation decrease with inflammation, while apical expression of IIA increases with inflammation, and there is a negative correlation between these signals. Myosin and actin form a dense ring that encircles the cell at the level of the adherens junction and TJ. Activation of actomyosin contraction, as assessed by phosphorylation of myosin II regulatory light chain (MLC), has been implicated in TJ regulation (23, 24). Notably, NMIIA plays an important role

in modulating transcription factor expression and activity by interacting with TNFR2 and modulating the Akt/GSK3-NF- $\kappa$ B signaling pathways to inhibit thrombosis (25). Therefore, NMIIA may be an important target in inflammation treatment.

Steroidal saponin DT-13 (25(R,S)-ruscogenin-1-O-[[ $\beta$ -D-glucopyranosyl-(1 $\rightarrow$ 2)]] $\beta$ -D-xylopyranosyl-(1 $\rightarrow$ 3)]]- $\beta$ -D-fucopyranoside) (Figure S1A in Supplementary Material), one of the active compounds isolated from *Liriope muscari*, has been shown to have various biological properties, including anti-inflammatory, cardioprotective, and antitumor activities (26–28). Recently, it was reported that DT-13 inhibited the phosphorylation of Src (Tyr416) in TNF- $\alpha$ -induced human umbilical vein endothelial cells (HUVECs) and could be safely used as a potential drug for vascular inflammation (29). DT-13 attenuated human lung cancer metastasis by regulating NMIIA activity under hypoxic conditions (30–32). However, it is not clear whether DT-13 plays a role in ameliorating vascular permeability.

Thus, in the present study, we showed that TNF- $\alpha$  significantly enhanced permeability in endothelial cells *via* a signaling pathway involving Src and PI3K/Akt, which led to the disruption of TJ proteins, such as ZO-1, and barrier dysfunction in the endothelial cells. These findings provide novel insight into the effect of DT-13 on endothelial barrier function, which is critical in vascular hyperpermeability-associated diseases. NMIIA may play an important role in the DT-13-mediated protection of against endothelial cell dysfunction.

## MATERIALS AND METHODS

### Extraction and Isolation of DT-13

DT-13 was isolated as previously described and identified as (25(R,S)-ruscogenin-1-O-[[ $\beta$ -D-glucopyranosyl-(1 $\rightarrow$ 2)]] $\beta$ -D-xylopyranosyl-(1 $\rightarrow$ 3)]]- $\beta$ -D-fucopyranoside) by comparison of its physical data (1H NMR, 13C NMR, MS) with published values. The purity of DT-13 was shown to be 98.5% using HPLC–ELSD assays as previously reported (33).

### Cell Culture

Human umbilical vein endothelial cells were purchased from the Shanghai Institute of Cell Biology, Chinese Academy of Sciences. HUVECs were grown in RPMI 1640 medium (Invitrogen Life Technologies, Carlsbad, CA, USA) supplemented with 10% heat-inactivated fetal bovine serum (FBS, ScienCell, CA, USA), 100 U/mL penicillin, 100  $\mu$ g/mL streptomycin, and 2.0 g/L sodium bicarbonate. Cells were maintained at 37°C with 95% humidity and 5% CO<sub>2</sub>.

### Vascular Permeability Assay

Ten-week-old male C57BL/6 mice were purchased from Yangzhou University (Yangzhou, China, certificate NO. SCXK 2014-0004). Mice were housed in microisolator cages in a pathogen-free facility. Evans blue dye (30 mg/kg) in 100  $\mu$ L PBS (Evans blue, Sigma, USA) was injected into the tail vein. After 1 min, mustard oil (Sigma, USA) diluted to 5% in sunflower seed oil was applied to the dorsal and ventral surfaces of the ear as described in previous studies (34). This process was repeated 15 min later. Then,

photographs were taken 30 min after injection of Evans blue dye. After the mice were euthanized, the ears were removed, blotted dry, and weighed. The Evans blue dye was extracted from the ears with 1 mL of formamide overnight at 55°C, and the OD value at 600 nm was determined. All animal experimental procedures and welfare were in accordance to National Institutes of Health Guide for the Care and Use of Laboratory Animals, and the protocols used were approved by the Animal Ethics Committee of China Pharmaceutical University, China Pharmaceutical University, Nanjing, China.

## Animals and Experimental Design

After an initial acclimation period, the mice were randomly divided into four groups, with six mice per group. Mice were pre-treated with DT-13 by intragastric administration with 4.0 mg/kg for 1 h. After 1 h, the mice were administered TNF- $\alpha$  by intraperitoneal injection with 100  $\mu$ g/kg for 4 h. Mice received saline (0.9%), DT-13 or dexamethasone (Dex) for the same period. At the end of the experimental period, all mice were euthanized 2 h after the last TNF- $\alpha$  injection. Blood samples were collected, and serum was frozen at  $-80^{\circ}\text{C}$  for the ELISA analysis.

## Immunofluorescence Staining

The immunofluorescence staining of ZO-1 *in vivo* was determined as described previously with a few modifications (35). Aortas from the mice were rapidly excised under general anesthesia, carefully trimmed to remove fat and connective tissue and washed twice by ice-cold PBS. Then the aortas were opened longitudinally to expose the endothelium and pinned onto 4% agar. HUVECs were cultured to confluence on glass cover slips in complete media containing 10% FBS and maintained for 7 days. Cells were then stimulated with TNF- $\alpha$  (10 ng/mL) for 4 h with or without prior treatment with DT-13 (1  $\mu$ M) for 1 h. The aortas or cells were washed with PBS and fixed in 4% formaldehyde in PBS (v/v) for 30 min at room temperature, and permeabilized in 0.1% Triton X-100 in 5% bovine serum albumin (BSA, diluted in PBS) for 30 min at room temperature. The aortas or cells were then blocked with 5% BSA for 1 h at room temperature. Then, they were incubated with rabbit anti-ZO-1 polyclonal antibody overnight at 4°C and washed with PBS three times followed by incubation with donkey antirabbit IgG 488-conjugated secondary antibody for 1 h. All samples were assessed using a fluorescence microscope (LSM700, Zeiss, Germany).

## Transendothelial Electrical Resistance (TEER) Assays and Sodium Fluorescein (Na-F) Assays

Human umbilical vein endothelial cells were seeded on transwell inserts (0.4  $\mu$ M pore, 6.5 mm diameter, Millipore, USA) for 7 days. The TEER of the monolayer was also measured daily with a Millicell-ERS voltohmmeter (Millipore, USA). Resistance values of multiple transwell inserts of an experimental group were measured sequentially, and the mean was expressed in the common unit ( $\Omega\cdot\text{cm}^2$ ) after subtraction of the value of a blank cell-free filter. The TEER of the monolayers was recorded when a stable resistance reading was achieved with triplicate measurements that were taken for each transwell. DT-13 (0.01–1  $\mu$ M) or Dex

(1  $\mu$ M) was added to the upper chamber for 1 h, and 10 ng/mL TNF- $\alpha$  (Bioworld, USA) was added for 4 h. Paracellular permeability was assessed by the addition of Krebs–Ringer buffer (118 mM NaCl, 4.7 mM KCl, 1.3 mM  $\text{CaCl}_2$ , 1.2 mM  $\text{MgCl}_2$ , 1.0 mM  $\text{NaH}_2\text{PO}_4$ , 25 mM  $\text{NaHCO}_3$ , and 11 mM D-Glucose, pH 7.4) containing 100  $\mu$ g/mL Na-F to the top chamber. The fluorescence was measured after 30 min at 37°C. The Na-F concentration was determined using a fluorescence multiwell plate reader [Ex ( $\lambda$ ) 485 nm; Em ( $\lambda$ ) 530 nm; Thermo].

## Transmission Electron Microscopy (TEM)

For direct examination of the ultrastructural characteristics of TJs, HUVECs were prepared using standard techniques and examined under a TEM (JEM1230, JEOL). Briefly, after fixation for 2 h with cold 2.5% glutaraldehyde and after several washes in 0.1 M PBS, the cells were gently scraped from the glass slides and pelleted by centrifugation. Cells were then post-fixed with 1% osmium tetroxide for 1 h at 4°C and stained en bloc with 2% uranyl acetate for an additional 1 h. After three more washes in double-distilled water, the samples were dehydrated in a series of acetone solutions and embedded in Epon 812 using a standard procedure. Random fields taken from individual endothelial cells samples were photographed at  $\times 30,000$ .

## Reverse Transcription Quantitative Polymerase Chain Reaction (RT-PCR)

Human umbilical vein endothelial cells were seeded overnight at  $3.0 \times 10^5$  cells/dish. The cells were treated with or without DT-13 at a concentration of 1  $\mu$ M for 1 h before exposure to TNF- $\alpha$  for 4 h. After cell stimulation, total RNA (four samples from each treatment group) was extracted using TRIzol reagent following the manufacturer's protocol (Sunshine Biotechnology, Nanjing, China). Reverse transcription was performed using a First Strand cDNA synthesis kit (Vazyme, China), and qPCR was performed using SYBR Green Supermix (Bio-Rad, USA). The primer sequences used in RT-PCR were as follows: human 18 S, 5'-CAGCCACCCGAGATTGAGCA-3' and 5'-TAGTAGCGACGGCGGTGTG-3'; ZO-1, 5'-GCCTAATCTGACCTATGAAC-3' and 5'-GGACTCGTATCTGTATGTG-3'. The amplification conditions were one cycle of 95°C for 30 s followed by 39 cycles of 95°C for 5 s, and 58°C for 15 s. mRNA expression was normalized to the level of 18 S expression. Changes in mRNA expression were calculated according to the  $2^{-\Delta\Delta\text{CT}}$  method, where  $\Delta\text{CT} = \text{CT}_{\text{target gene}} - \text{CT}_{18\text{s}}$ , and  $\Delta\Delta\text{CT} = \text{CT}_{\text{treatment}} - \Delta\text{CT}_{\text{control}}$ , and CT is the value for cycle threshold.

## Western Blotting

Human umbilical vein endothelial cells were handled with various concentrations (0.01, 0.1, and 1  $\mu$ M) of DT-13 for 1 h following TNF- $\alpha$  (10 ng/mL) stimulation for 4 h. After the cells were washed with PBS, they were lysed using lysis buffer (containing 20 mM Tris, pH 7.5, 1% Triton X-100, 150 mM NaCl, sodium pyrophosphate,  $\beta$ -glycerophosphate, EDTA,  $\text{Na}_3\text{VO}_4$ , leupeptin) for 30 min on ice. Protein concentration was measured using a BCA protein assay kit. Equal amounts of protein (40  $\mu$ g) were separated using SDS-PAGE and then transferred onto a PVDF membrane. The membrane was then blocked with 3% BSA for

1.5 h, followed by overnight incubation at 4°C in the primary antibody. After the membrane was washed, a HRP-conjugated secondary antibody was added and incubated for 1.5 h. The bands were detected by an ECL kit and quantified by Quantity One software.

### siRNA Transfection

Non-muscle myosin IIA siRNA and control non-specific siRNA were purchased from Biomics Biotechnologies Co. (Nantong, China). Transfection of cells with the siRNAs was performed using ExFect Transfection Reagent (Vazyme, China) according to the manufacturer's instructions. Briefly, the endothelial cells were plated on a 60 mm dish at a concentration of  $5 \times 10^5$  cells/dish. After reaching 50% confluence, the cells were transfected with the siRNA for 48 h and treated with DT-13 (0.01, 0.1, 1  $\mu$ M) for 1 h followed by a 4 h treated with TNF- $\alpha$  (10 ng/mL) at 37°C. The siNMIIA sequences were as follows: forward, 5'-GAGGCAAUGAUCACUGACUdTdT-3'; reverse, 5'-AGUCAGUGAUCAUUGCCUCdTdT-3'. For analysis of the efficiency of protein suppression, total cell lysates were resolved by SDS-PAGE for immunoblotting with antibodies against GAPDH (Kangchen, China) and NMIIA (CST).

### Pose Validation, Molecular Preparation, and Docking

The protein docking was determined as described previously with a few modifications (36). Considering different state and sequences of the myosin models, the binding cavity was found by assistant methods based on the literature data (37). The precise binding cavity was determined *via* CH3 probe by Q-sitefinder [SP5] and blind docking by Autodock3.05 [SP6]. The steps were as follows: DT-13 and homology model of NMMHC IIA were prepared using ligprep and protein preparation wizard in Maestro 8.0 [SP7] adding hydrogen atoms and desalting. The next step comprised the grid generation performed by box size (32 Å  $\times$  32 Å  $\times$  32 Å). In this step, a distinct area of the structure was defined, in which the docking was performed. The grid box was manually positioned to comprise the whole ligand-binding site. The docking step was performed using the generated grid files and the prepared ligands, with the advanced option set as 14 Å  $\times$  14 Å  $\times$  14 Å. The initial complex conformation was subjected to further molecular minimization by Gromacs3.3 on an IBM system X3400 server in the AMBER03 force field environment. Topology parameters were self-generated by the Dundee Prodr2 server. The same steps described for optimizing protein alone were also used for bound complexes. Molecular graphics were inspected in molecular virtual viewer1.2.0 (Molegro) [SP8] and Discovery Studio.

### Statistical Analysis

GraphPad Prism software (Version 4.0, GraphPad Software, Inc., San Diego, CA, USA) was used to perform the data analysis. Data are expressed as the mean  $\pm$  SD. Statistical significance between different groups was calculated by a one-way ANOVA where appropriate or a Student's two-tailed *t*-test; *P*-values below 0.05 were considered statistically significant.

## RESULTS

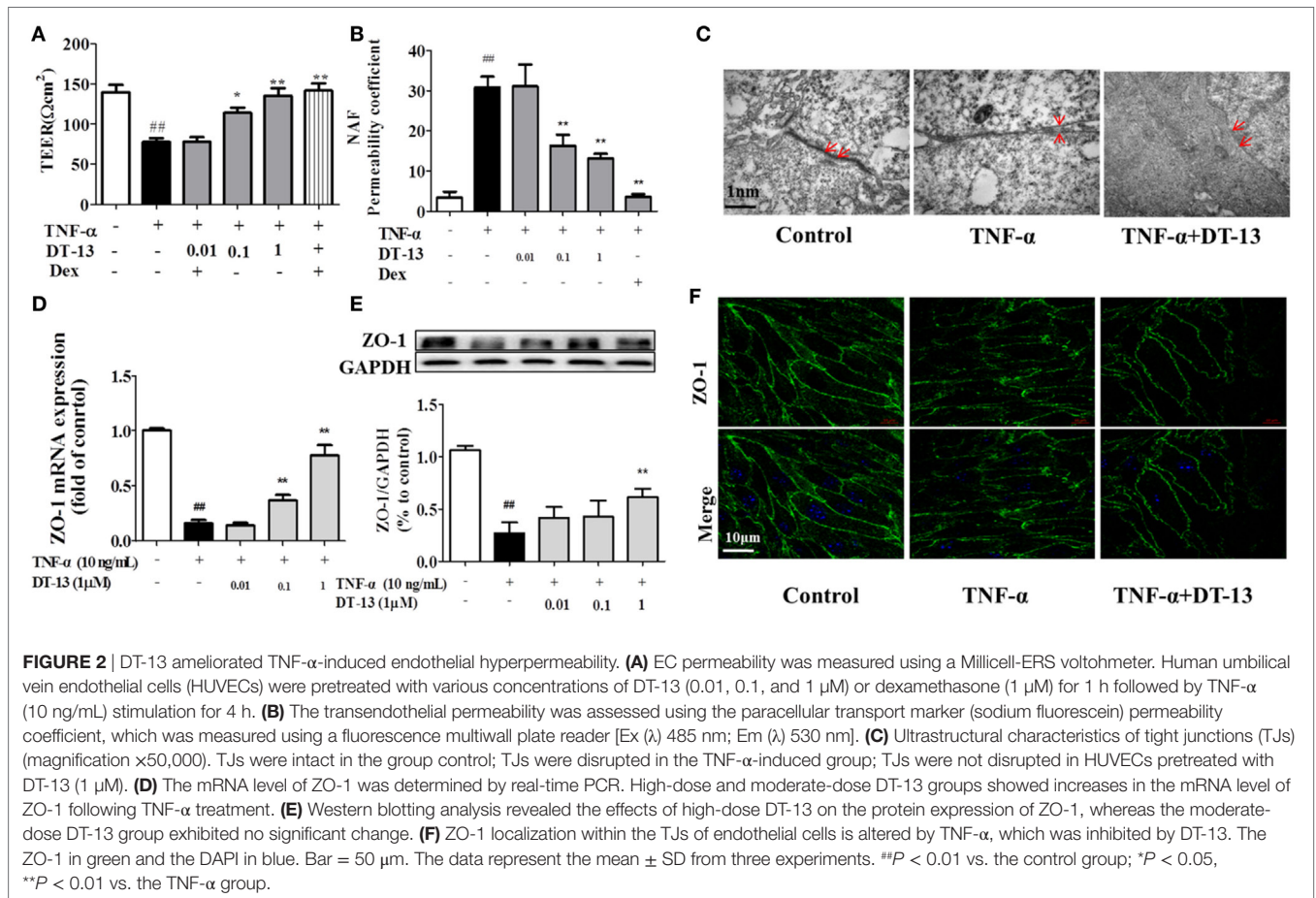
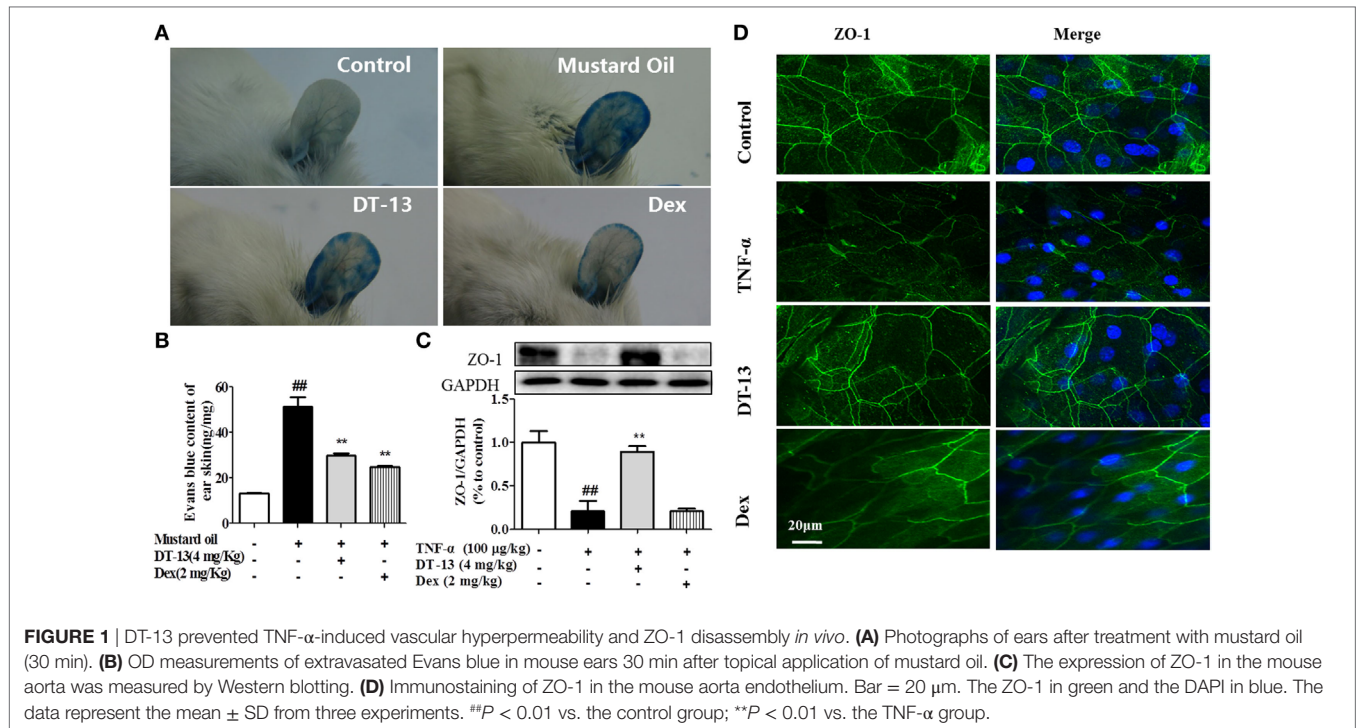
### Effect of DT-13 on Vascular Permeability and ZO-1 Organization *In Vivo*

Dexamethasone was used in this part as a positive control to identify the successful construction of model *in vivo*. The response of vessels to mustard oil, an inflammatory agent that induces plasma leakage and inflammation in the skin, was examined. After injection of Evans blue dye and application of mustard oil, the ears of control mice became moderately blue. The ears of TNF- $\alpha$ -stimulated mice became completely blue, particularly at the periphery. In contrast, the ears of mice treated with DT-13 remained pale (Figure 1A). The group treated with Dex remained pale. Evans blue OD analysis revealed that leakage increased fourfold in TNF- $\alpha$ -stimulated mice. However, leakage did not increase significantly in the ear skin of mice treated with DT-13 and Dex (Figure 1B). As shown in Figure 1C, mice were pretreated with DT-13 (4.0 mg/kg) or Dex (2.0 mg/kg) for 1 h and then administered TNF- $\alpha$  (100  $\mu$ g/kg) for 4 h. The protein expression of ZO-1 was significantly increased compared with that of the model group. Immunostaining of ZO-1 in the mouse aorta endothelium showed that TNF- $\alpha$  abolished the endothelial junctional protein at the cell-cell contact zones between adjacent cells. DT-13 (4.0 mg/kg) inhibited ZO-1 disassembly (Figure 1D). Notably, DT-13 was as potent as the glucocorticoid Dex.

### Effect of DT-13 on Endothelial Monolayer Permeability and Ultrastructural Characteristics of TJs *In Vitro*

The effects of TNF- $\alpha$  or DT-13 on HUVEC monolayer permeability were examined by detecting the TEER of the EC monolayer and performing transwell Na-F assays. DT-13 at concentrations of 0.01, 0.1, and 1  $\mu$ M was applied for 1 h, followed by TNF- $\alpha$  stimulation for 4 h. DT-13 or TNF- $\alpha$  had no effect on HUVEC viability (Figure S1B in Supplementary Material). TEER was reduced in the TNF- $\alpha$  group and DT-13 (1  $\mu$ M) group by 42.3 and 0.3%, respectively (Figure 2A). TNF- $\alpha$ -induced barrier disruption resulted in a sharp decrease in TEER and an increase in the Na-F permeability coefficient. However, DT-13 enhanced TEER and decreased the Na-F permeability coefficient (Figure 2B). As a positive control, 1  $\mu$ M Dex protected endothelial cell permeability. In the control group, the endothelial cells were tightly arranged. In contrast, large intercellular gaps were observed after TNF- $\alpha$  stimulation. However, the structure in the DT-13 group was undisrupted (Figure 2C).

Downregulation of the TJ protein ZO-1 may be critical for disruption of the endothelial barrier (13). This protein showed discrete localization in response to TNF- $\alpha$  treatment; however, ZO-1 in HUVECs treated with DT-13 was intact, in contrast to the group model. HUVECs were exposed to TNF- $\alpha$  and assessed for the expression of ZO-1 by RT-qPCR and Western blot analyses. As shown in Figures 2D,E, treatment of the HUVECs with TNF- $\alpha$  decreased the protein and mRNA expression of ZO-1, and this effect was significantly ameliorated in HUVECs pretreated with DT-13 at 1  $\mu$ M. The ZO-1 protein maintains the structural integrity of TJs in endothelial cells. Using immunofluorescence,



we identified the localization of ZO-1 at the endothelial cell contacts of confluent cells (Figure 2F).

### Effect of DT-13 on TNF- $\alpha$ -Induced Src/PI3-Kinase/Akt Pathway

Pro-inflammatory cytokines increase the permeability and disassembly of ZO-1 *via* the PI3K/Akt pathway (38). Figure 3 shows that TNF- $\alpha$  increased Src, PI3K, and Akt phosphorylations in HUVECs. DT-13 dose-dependently blocked TNF- $\alpha$ -induced Src phosphorylation (Tyr416) and simultaneously abolished TNF- $\alpha$ -induced PI3K and Akt phosphorylation.

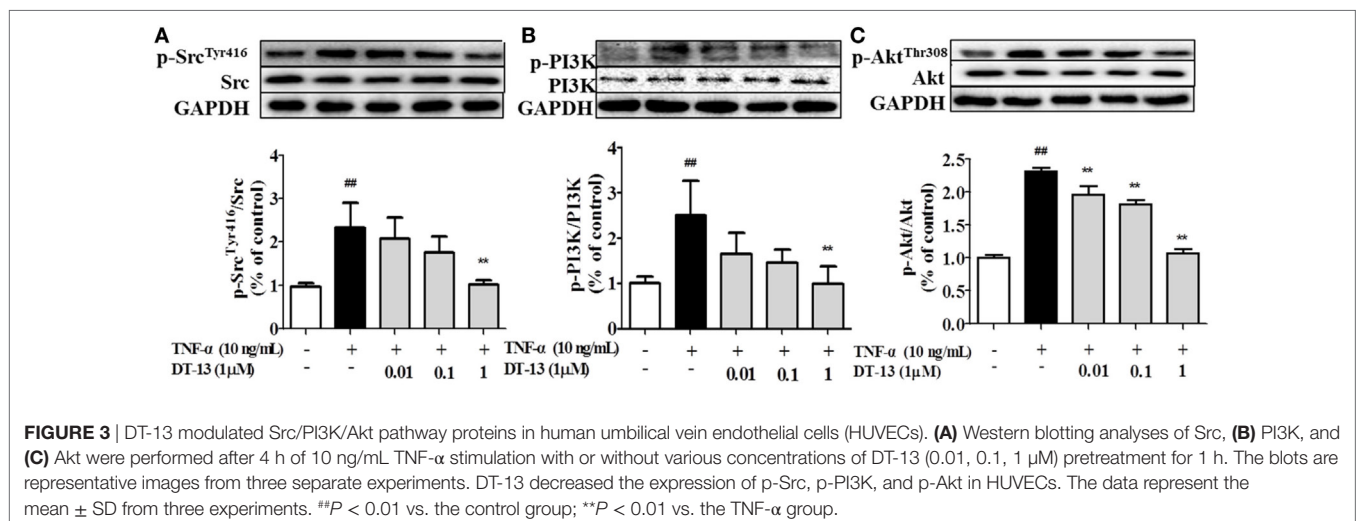
### DT-13 Attenuates TNF- $\alpha$ -Induced Disassembly Mediated by the Src/PI3-Kinase/Akt Pathway

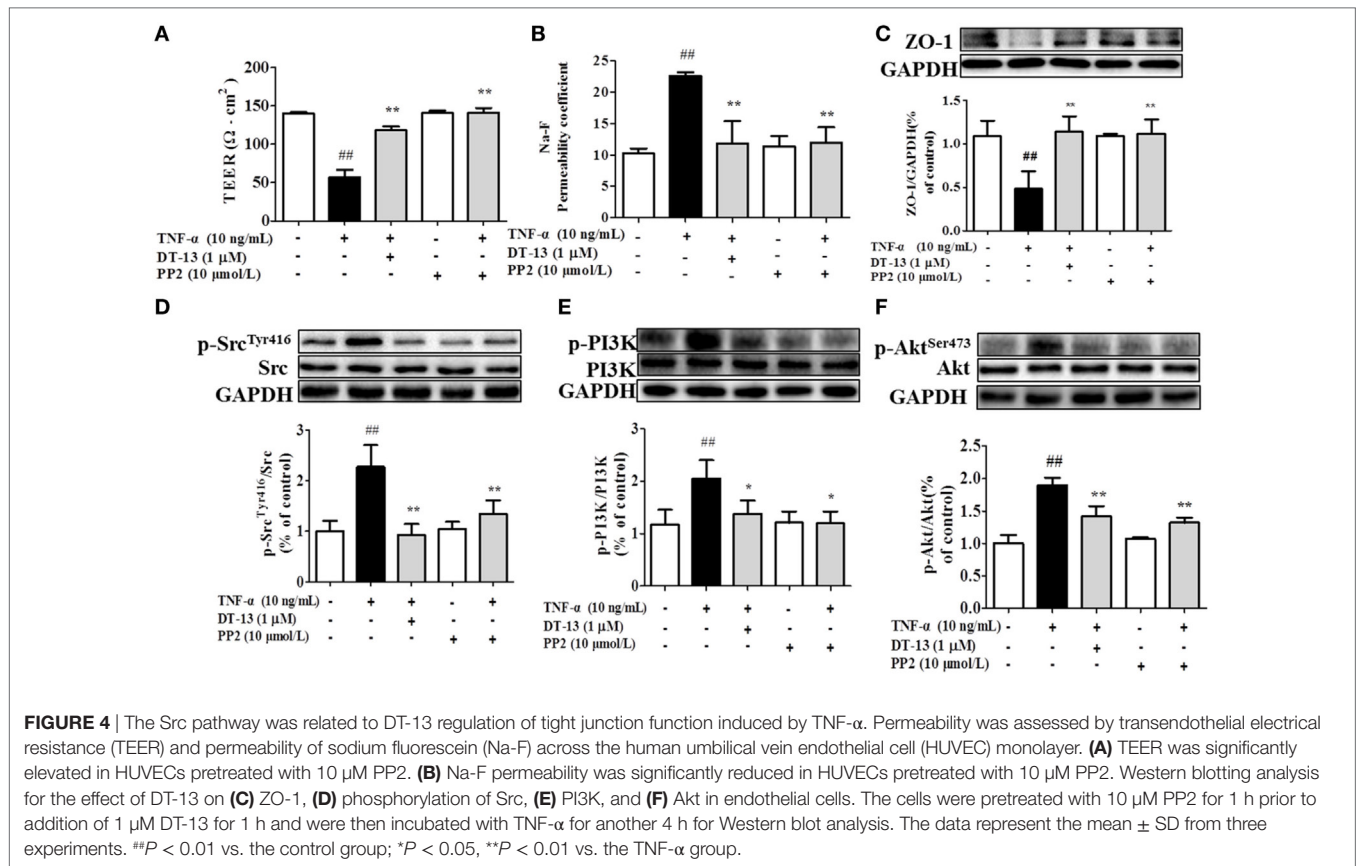
Src family kinase activity was also shown to be important for TNF- $\alpha$ -mediated stimulation of PI3K/AKT activity because an Src inhibitor significantly prevented this. To determine the significance of Src, we carried out permeability studies. After HUVECs were pretreated with PP2 for 24 h, TEER values and the Na-F permeability coefficient were detected. TEER values in the TNF- $\alpha$  + PP2 groups were significantly increased compared with those in the TNF- $\alpha$  group (Figure 4A), and the Na-F permeability coefficient decreased (Figure 4B). Endothelial permeability is regulated in part by the endothelial cell-cell TJs, which are largely composed of ZO-1 (39). We hypothesized that DT-13 may decrease vascular permeability *via* an Src-induced disruption of ZO-1 localization to endothelial cell junctions. As expected, in control cells, ZO-1 was highly expressed (Figures 4C,D). Following treatment with 10 ng/mL TNF- $\alpha$ , lower levels of ZO-1 were found. However, pretreatment with the Src inhibitor PP2 (10  $\mu$ M) for 1 h prior to TNF- $\alpha$  blocked the disassembly of ZO-1 (40). Inhibition of Src or DT-13 in HUVECs reduced the phosphorylations of Src, PI3K, and Akt. The cells were pretreated with the PI3K inhibitor LY294002 (10  $\mu$ M) for 1 h prior to TNF- $\alpha$ , and TEER values and the Na-F permeability coefficient were detected (Figures 5A,B). TEER values in the TNF- $\alpha$  + LY294002

group were significantly increased compared with those in the TNF- $\alpha$  group. The Na-F permeability coefficient decreased. The expression of p-PI3K was decreased compared with that of the model group. However, in the same condition, the expression of p-Src was not significantly different from that of the model group (Figures 5C,D).

### NMIIA Plays an Important Role in DT-13-Attenuated TNF- $\alpha$ -Induced Endothelial Hyperpermeability and Related Pathways

Computer aided methods were then used to construct a virtual model of NMMHC IIA by homology modeling and to illuminate the possible binding sites and binding mode of DT-13. Based on receptor structure combined with docking pharmacophore virtual screening method with G-score (-6.5), it was found that the DT-13 might locate into the cleft region similar to the inhibitor of NMMHC IIA and interacted with various binding sites including functional domains of ATPase, actin-binding or tail area of NMMHC IIA. As shown in Figure 6C, the basal expression of p-Src (Tyr416) increased in the NMIIA KD group (the expression of NMIIA was knocked down by the siRNA shown in Figure S1C in Supplementary Material) compared with that of the control HUVECs. These results indicated that NMIIA KD increase Src phosphorylation at Tyr416. However, the DT-13-mediated inhibition of Src Tyr416 was reduced in NMIIA KD HUVECs. The NMIIA KD abolished the effect of DT-13 on Src Tyr 416 phosphorylation. As shown in Figure 6D, the basal expression of p-Akt (473) increased in NMIIA KD HUVECs. DT-13 inhibited Akt phosphorylation by 30%. However, there was no response to TNF- $\alpha$ -induction, and DT-13 did not inhibit p-Akt (473) expression in NMIIA KD HUVECs. As shown in Figure 6E, the basal expression of p-PI3K increased in NMIIA KD HUVECs. DT-13 could inhibit the PI3K phosphorylation by 41%. PI3K phosphorylation was stimulated by TNF- $\alpha$  in NMIIA KD cells. However, DT-13 did not inhibit p-PI3K expression in NMIIA KD cells. These result indicated that NMIIA is essential for the DT-13-mediated effect on the PI3K/Akt pathway.





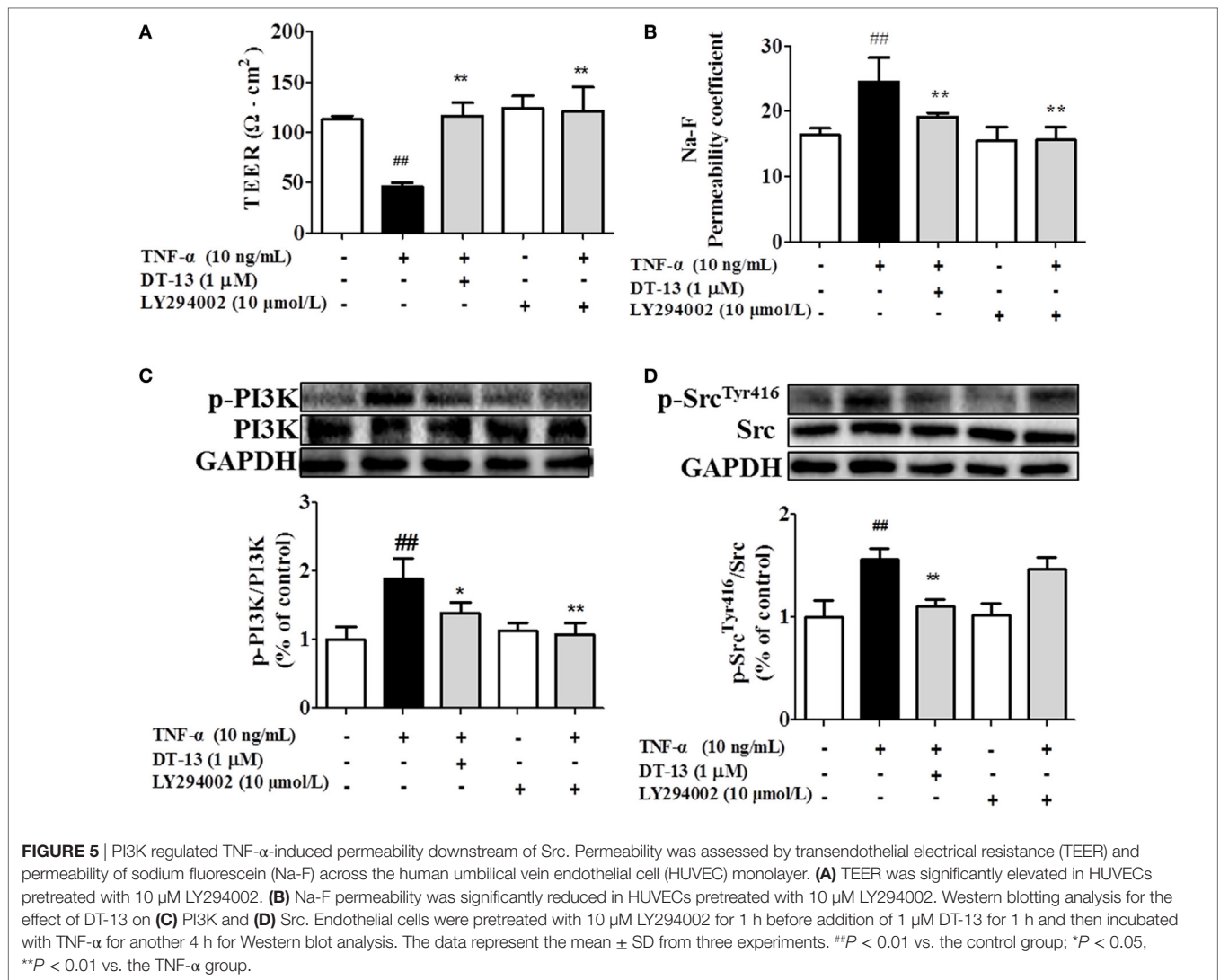
## DISCUSSION

In this study, we demonstrated that DT-13, one of the major active compounds of *L. muscari*, suppressed the increase in TNF- $\alpha$ -stimulated endothelial cell permeability and the disassembly of ZO-1, possibly due to inhibition of the PI3K/Akt signaling pathway by modulating Src activation. These findings provide pharmacological evidence for the protective effect of DT-13 in treating cardiovascular disease and cancer, and the underlying mechanisms may be *via* modulation of TJs through the Src/PI3K/Akt signaling pathway. Moreover, NMIIA is essential for DT-13-mediated protection of endothelial cell permeability.

Vascular injury leads to endothelial injury and structural damage to TJs, resulting in systemic inflammatory response syndrome and sepsis (41). Endothelial hyperpermeability is a common characteristic of many diseases, including inflammation, trauma, sepsis, ischemia-reperfusion injury, diabetes, and atherosclerosis (42–45). In ALI, the endothelial cell barrier is weakened, leading to increased vascular permeability (46). As a crucial event in the progression of atherosclerosis, disruption of endothelial TJs accounts for the majority of the cardiovascular disease-related deaths (47). The blood–brain barrier (BBB) and the blood retinal barrier (BRB) are particularly rich in endothelial TJs. BBB/BRB disruption results in central nervous system diseases. Vascular leakage not only causes multiorgan dysfunction but also compromises the normal pharmacokinetics of therapeutic drugs (48).

The inflammatory agent mustard oil is known to cause plasma leakage *via* increased numbers of leakage sites in the endothelium in mouse skin (49). In this study, mustard oil was used to induce hyperpermeability *in vivo*. TNF- $\alpha$ -induced vascular permeability is a critical contributor to the pathophysiology of vascular insufficiency (50). Pro-inflammatory mediators and neutrophils induced vascular hyperpermeability by Src signaling (51). Studies have showed that oxidants, VEGF, thrombin, neutrophils, and TNF- $\alpha$  increased Src activity in association with increased endothelial permeability (52, 53). TNF- $\alpha$  is a major pro-inflammatory cytokine that increases vascular permeability *via* disruption of intercellular junctions. Drugs can extravasate and accumulate inside the interstitial space; thus, their bioavailability and effectiveness are therefore reduced, and systemic toxicity can increase (54). In this report, we showed for the first time that DT-13 affects endothelial cell permeability induced by mustard oil *in vivo* and TNF- $\alpha$  *in vitro* (Figures 1 and 2). Therefore, we hypothesize that DT-13 may play a cardioprotective, antitumor, anti-inflammatory, and antistroke role *via* the effect on TJs (Figure 1).

ZO-1 is essential for the proper assembly of endothelial junction complexes that control endothelial junctional barrier integrity (55). TNF- $\alpha$  decreased the protein and mRNA content of the TJ protein ZO-1 and altered the endothelial cell permeability. The total content of the TJ protein ZO-1 under experimental conditions was determined by Western blotting

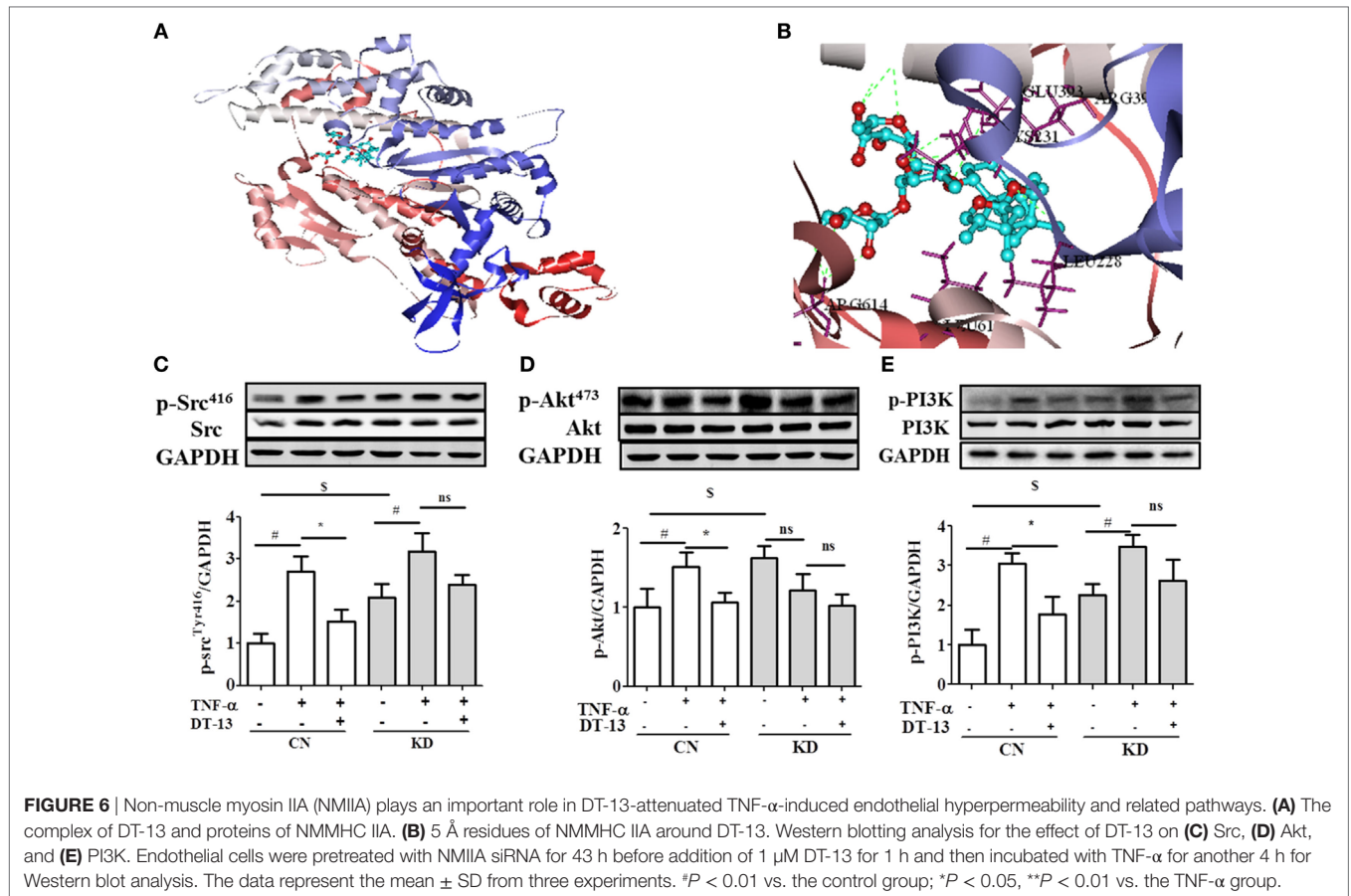


and RT-PCR. Pretreatment with DT-13 increased TEER and up-regulated ZO-1. DT-13 was shown to enhance vascular TJ barrier integrity by up-regulation and rearrangement of ZO-1 (Figures 1 and 2).

Recent studies have elucidated the mechanisms by which Src family kinases regulate normal and pathological processes in vascular biology, including endothelial cell proliferation and permeability (56). There were reports indicated that Src tyrosine kinases promote inflammatory processes under various pathological conditions induced by TNF- $\alpha$  (57). Activation of PI3K appears to occur *via* phosphorylation of tyrosine residues in Src, which permits docking of PI3K to the plasma membrane and allows allosteric modifications that increase its catalytic activity (58). The Src inhibitor PP2 blocked the PI3K/Akt-mediated alteration in ZO-1 expression (59). Pretreatment with the PI3K inhibitor LY294002 blocked alteration in ZO-1 expression. Inhibition of Src in TNF- $\alpha$ -treated HUVECs decreased permeability and up-regulated expression of the endothelial cell TJ protein ZO-1, and this effect was mediated by inhibition

of PI3K/Akt signaling (60). Our results indicated that DT-13 enhances vascular TJ barrier integrity through a mechanism involving Src and the PI3K/Akt pathway. Together, our data showed that DT-13 decreased endothelial cell permeability by enhancing endothelial cell TJ protein expression and that the Src/PI3K/Akt signal pathway is involved in this process (shown in Figures 3–5).

Myosin and actin form a dense ring that encircles the cell at the level of the adherens junction and TJ. The results of the docking-based virtual screening showed that NMIIA may be the combined protein of DT-13. Activation of actomyosin contraction, as assessed by phosphorylation of MLC, has been implicated in TJ regulation (23, 24). KD studies have shown that NMIIA activation is necessary for TJ response to diverse physiological and pathophysiological stimuli (61). Our data indicated that blocking NMIIA activation in HUVECs is sufficient to inhibit the effect of DT-13 on the Src/PI3K/Akt pathway. In this study, the expression of NMIIA was inhibited by siRNA, and the effect of DT-13 on the Src/PI3K/Akt signaling pathway was decreased.



These results suggest that the regulatory effect of DT-13 on the Src/PI3K/Akt signaling pathway was closely related to NMIIA (shown in **Figure 6**). Thus, NMIIA may mediate DT-13 regulation of the Src/PI3K/Akt signaling pathway to improve endothelial hyperpermeability.

The major aim of the present study was to investigate the effect of DT-13 on TNF- $\alpha$ -induced endothelial hyperpermeability. Natural products have long been recognized as a key source for the development of novel therapeutic strategies to treat human disorders, including inflammatory diseases. Tongxinluo, a traditional Chinese medicinal compound, increased TJ protein expression after chronic hypoxia both *in vivo* and *in vitro* (62). He-Ying-Qing-Re Formula, a well-known traditional Chinese medicine, was shown to protect endothelial dysfunction *via* modulation of TJs (63). We demonstrated for the first time that DT-13 suppressed the increase in TNF- $\alpha$ -stimulated EC permeability and the disassembly of ZO-1, possibly due to inhibition of the PI3K/Akt signaling pathway by modulating Src activation. NMIIA may be the key mediator of DT-13-induced endothelial hyperpermeability amelioration. Moreover, we demonstrated that DT-13 could improve vascular barrier function. Thus, DT-13 could be developed as a drug to treat diseases related to vascular dysfunction, such as hypertension, stroke, and others.

Our results first confirmed that NMIIA has played an important role in the DT-13-mediated effect on the Src/PI3K/

Akt pathway. As reported, saponin compounds from Chinese herbal could be the inhibitor of NM IIA based on combined pharmacophore- and docking-based virtual by computer calculation (36). However, further studies are needed to explore. First, the effect of DT-13 on the NM IIA ATPase activity needed to be investigated in future studies. Second, how the conditional NMIIA-KO in endothelial cells contributes in vascular barrier function requires further study. On the other hand, our results indicated that DT-13 enhances vascular TJ barrier integrity through a mechanism involving Src and the PI3K/Akt pathway as determined using the Src inhibitor PP2 and PI3K inhibitor LY294002. KD or knock out studies of Src and PI3K should be performed in the future.

Overall, our findings provide pharmacological evidence supporting the protective effect of DT-13 in treating cardiovascular disease and cancer. The underlying mechanisms are mediated *via* modulation of TJs through the Src/PI3K/Akt signaling pathway. More importantly, we demonstrated that NMIIA was essential in the process of DT-13-improved endothelial hyperpermeability. Our results provide new insights into the effects and mechanisms of DT-13 on endothelial hyperpermeability, which play an important role for the onset and progression of cardiovascular diseases, such as atherosclerosis, cancer, and stroke. Therefore, DT-13 may be a potential candidate drug for immunology disease intervention.

## ETHICS STATEMENT

All animal welfare and experimental procedures were in accordance with National Institutes of Health Guide for the Care and Use of Laboratory Animals, and the protocols used were approved by the Animal Ethics Committee of China Pharmaceutical University, China Pharmaceutical University, Nanjing, China.

## AUTHOR CONTRIBUTIONS

YZhang analyzed the data, wrote, discussed, and reviewed the manuscript. YHan wrote the manuscript and performed the experiments *in vivo* and intro. YZhao performed the experiments *in vivo* and intro. YL and YT performed the experiments in Pose validation, molecular preparation, and docking. YHu and XB performed the experiments *in vitro*. BY and JK discussed and reviewed the manuscript.

## REFERENCES

- Lee WL, Slutsky AS. Sepsis and endothelial permeability. *N Engl J Med* (2010) 363(7):689–91. doi:10.1056/NEJMcibr1007320
- Alvarez-Sabin J, Maisterra O, Santamarina E, Kase CS. Factors influencing haemorrhagic transformation in ischaemic stroke. *Lancet Neurol* (2013) 12(7):689–705. doi:10.1016/S1474-4422(13)70055-3
- de Punder K, Pruijboom L. Stress induces endotoxemia and low-grade inflammation by increasing barrier permeability. *Front Immunol* (2015) 6:223. doi:10.3389/fimmu.2015.00223
- Rodrigues SF, Granger DN. Blood cells and endothelial barrier function. *Tissue Barriers* (2015) 3(1–2):e978720. doi:10.4161/21688370.2014.978720
- Balda MS, Matter K. Tight junctions as regulators of tissue remodelling. *Curr Opin Cell Biol* (2016) 42:94–101. doi:10.1016/j.cob.2016.05.006
- Yu J, Ma M, Ma Z, Fu J. HDAC6 inhibition prevents TNF- $\alpha$ -induced caspase 3 activation in lung endothelial cell and maintains cell-cell junctions. *Oncotarget* (2016) 7(34):54714–22. doi:10.18632/oncotarget.10591
- Good RB, Gilbane AJ, Trinder SL, Denton CP, Coghlan G, Abraham DJ, et al. Endothelial to mesenchymal transition contributes to endothelial dysfunction in pulmonary arterial hypertension. *Am J Pathol* (2015) 185(7):1850–8. doi:10.1016/j.ajpath.2015.03.019
- Tsukita S, Furuse M, Itoh M. Multifunctional strands in tight junctions. *Nat Rev Mol Cell Biol* (2001) 2(4):285–93. doi:10.1038/35067088
- Umeda K, Ikenouchi J, Katahira-Tayama S, Furuse K, Sasaki H, Nakayama M, et al. ZO-1 and ZO-2 independently determine where claudins are polymerized in tight-junction strand formation. *Cell* (2006) 126(4):741–54. doi:10.1016/j.cell.2006.06.043
- Tada Y, Yagi K, Kitazato KT, Tamura T, Kinouchi T, Shimada K, et al. Reduction of endothelial tight junction proteins is related to cerebral aneurysm formation in rats. *J Hypertens* (2010) 28(9):1883–91. doi:10.1097/HJH
- Watters AK, Rom S, Hill JD, Dematatis MK, Zhou Y, Merkel SF, et al. Identification and dynamic regulation of tight junction protein expression in human neural stem cells. *Stem Cells Dev* (2015) 24(12):1377–89. doi:10.1089/scd.2014.0497
- Kiener TK, Slepsova-Friedrich I, Hunziker W. Identification, tissue distribution and developmental expression of tjp1/zo-1, tjp2/zo-2 and tjp3/zo-3 in the zebrafish, *Danio rerio*. *Gene Expr Patterns* (2007) 7(7):767–76. doi:10.1016/j.modgep.2007.05.006
- Van Itallie CM, Fanning AS, Bridges A, Anderson JM. ZO-1 stabilizes the tight junction solute barrier through coupling to the perijunctional cytoskeleton. *Mol Biol Cell* (2009) 20(17):3930–40. doi:10.1091/mbc.E09-04-0320
- Migliaccio A, Castoria G, Di Domenico M, de Falco A, Bilancio A, Lombardi M, et al. Steroid-induced androgen receptor-oestradiol receptor beta-Src complex

## FUNDING

This study was supported by the National Natural Science Foundation of China (No. 81274131 & No. 81503295), the 2011 Programme for Excellent Scientific and Technological Innovation Team of Jiangsu Higher Education, and a Project Funded by the Priority Academic Programme Development of Jiangsu Higher Education Institutions.

## SUPPLEMENTARY MATERIAL

The Supplementary Material for this article can be found online at <http://journal.frontiersin.org/article/10.3389/fimmu.2017.00925/full#supplementary-material>.

**FIGURE S1 | (A)** The chemical structure of DT-13. **(B)** DT-13 showed no significant cytotoxicity on HUVECs at concentrations of 0.01–1  $\mu$ M. **(C)** NMIIA was knocked down by a specific siRNA.

**FIGURE S2 |** The abstract graph of this paper.

- triggers prostate cancer cell proliferation. *EMBO J* (2000) 19(20):5406–17. doi:10.1093/emboj/19.20.5406
- Basuroy S, Sheth P, Kuppuswamy D, Balasubramanian S, Ray RM, Rao RK. Expression of kinase-inactive c-Src delays oxidative stress-induced disassembly and accelerates calcium-mediated reassembly of tight junctions in the Caco-2 cell monolayer. *J Biol Chem* (2003) 278(14):11916–24. doi:10.1074/jbc.M211710200
- Thapa N, Choi S, Tan X, Wise T, Anderson RA. Phosphatidylinositol phosphate 5-kinase  $\gamma$  and phosphoinositide 3-kinase/Akt signaling couple to promote oncogenic growth. *J Biol Chem* (2015) 290(30):18843–54. doi:10.1074/jbc.M114.596742
- Zhou Y, Tu C, Zhao Y, Liu H, Zhang S. Placental growth factor enhances angiogenesis in human intestinal microvascular endothelial cells via PI3K/Akt pathway: potential implications of inflammation bowel disease. *Biochem Biophys Res Commun* (2016) 470(4):967–74. doi:10.1016/j.bbrc.2016.01.073
- Oh TW, Park KH, Jung HW, Park YK. Neuroprotective effect of the hairy root extract of *Angelica gigas* NAKAI on transient focal cerebral ischemia in rats through the regulation of angiogenesis. *BMC Complement Altern Med* (2015) 15:101. doi:10.1186/s12906-015-0589-4
- Newell-Litwa KA, Horwitz R, Lamers ML. Non-muscle myosin II in disease: mechanisms and therapeutic opportunities. *Dis Model Mech* (2015) 8(12):1495–515. doi:10.1242/dmm.022103
- Zhao B, Qi Z, Li Y, Wang C, Fu W, Chen YG. The non-muscle-myosin-II heavy chain Myh9 mediates colitis-induced epithelium injury by restricting Lgr5+ stem cells. *Nat Commun* (2015) 6:7166. doi:10.1038/ncomms8166
- Aguilar-Cuenca R, Juanes-Garcia A, Vicente-Manzanares M. Myosin II in mechanotransduction: master and commander of cell migration, morphogenesis, and cancer. *Cell Mol Life Sci* (2014) 71(3):479–92. doi:10.1007/s00018-013-1439-5
- Kumari S, Vardhana S, Cammer M, Curado S, Santos L, Sheetz MP, et al. T lymphocyte myosin IIA is required for maturation of the immunological synapse. *Front Immunol* (2012) 3:230. doi:10.3389/fimmu.2012.00230
- Berglund JJ, Riegler M, Zolotarevsky Y, Wenzl E, Turner JR. Regulation of human jejunal transmucosal resistance and MLC phosphorylation by Na(+)-glucose cotransport. *Am J Physiol Gastrointest Liver Physiol* (2001) 281(6):G1487–93.
- Wang F, Graham WV, Wang Y, Witkowski ED, Schwarz BT, Turner JR. Interferon-gamma and tumor necrosis factor-alpha synergize to induce intestinal epithelial barrier dysfunction by up-regulating myosin light chain kinase expression. *Am J Pathol* (2005) 166(2):409–19. doi:10.1016/S0002-9440(10)62264-X
- Zhai K, Tang Y, Zhang Y, Li F, Wang Y, Cao Z, et al. NMMHC IIA inhibition impedes tissue factor expression and venous thrombosis via Akt/

- GSK3beta-NF-kappaB signalling pathways in the endothelium. *Thromb Haemost* (2015) 114(1):173–85. doi:10.1160/TH14-10-0880
26. Qiu C, Jozsef L, Yu B, Yu J. Saponin monomer 13 of dwarf lilyturf tuber (DT-13) protects serum withdrawal-induced apoptosis through PI3K/Akt in HUVEC. *Biochem Biophys Res Commun* (2014) 443(1):74–9. doi:10.1016/j.bbrc.2013.11.056
  27. Zhang Y, Liu J, Kou J, Yu J, Yu B. DT-13 suppresses MDA-MB-435 cell adhesion and invasion by inhibiting MMP-2/9 via the p38 MAPK pathway. *Mol Med Rep* (2012) 6(5):1121–5. doi:10.3892/mmr.2012.1047
  28. Li H, Sun L, de Carvalho EL, Li X, Lv X, Khan GJ, et al. DT-13, a saponin monomer of dwarf lilyturf tuber, induces autophagy and potentiates anti-cancer effect of nutrient deprivation. *Eur J Pharmacol* (2016) 781:164–72. doi:10.1016/j.ejphar.2016.04.016
  29. Zhang Y, Sun M, Han Y, Zhai K, Tang Y, Qin X, et al. The saponin DT-13 attenuates tumor necrosis factor-alpha-induced vascular inflammation associated with Src/NF-small ka, CyrillicB/MAPK pathway modulation. *Int J Biol Sci* (2015) 11(8):970–81. doi:10.7150/ijbs.11635
  30. Yu XW, Lin S, Du HZ, Zhao RP, Feng SY, Yu BY, et al. Synergistic combination of DT-13 and topotecan inhibits human gastric cancer via myosin IIA-induced endocytosis of EGF receptor in vitro and in vivo. *Oncotarget* (2016) 7(22):32990–3003. doi:10.18632/oncotarget.8843
  31. Wei XH, Lin SS, Liu Y, Zhao RP, Khan GJ, Du HZ, et al. DT-13 attenuates human lung cancer metastasis via regulating NMIIA activity under hypoxia condition. *Oncol Rep* (2016) 36(2):991–9. doi:10.3892/or.2016.4879
  32. Du H, Huang Y, Hou X, Yu X, Lin S, Wei X, et al. DT-13 inhibits cancer cell migration by regulating NMIIA indirectly in the tumor microenvironment. *Oncol Rep* (2016) 36(2):721–8. doi:10.3892/or.2016.4890
  33. Chen LL, Yuan WW, Hu ZF, Qi J, Zhu DN, Yu BY. Determination and pharmacokinetics of DT-13 in rat plasma by LC-MS. *J Pharm Biomed Anal* (2011) 56(3):650–4. doi:10.1016/j.jpba.2011.07.003
  34. Chen SC, Liu CC, Huang SY, Chiou SJ. Vascular hyperpermeability in response to inflammatory mustard oil is mediated by Rho kinase in mice systemically exposed to arsenic. *Microvasc Res* (2011) 82(2):182–9. doi:10.1016/j.mvr.2011.06.001
  35. Hakanpaal L, Sipila T, Leppanen VM, Gautam P, Nurmi H, Jacquemet G, et al. Endothelial destabilization by angiopoietin-2 via integrin beta1 activation. *Nat Commun* (2015) 6:5962. doi:10.1038/ncomms6962
  36. Lv Y, Lu S, Lu T, Kou J, Yu B. Homology model of nonmuscle myosin heavy chain IIA and binding mode analysis with its inhibitor blebbistatin. *J Mol Model* (2013) 19(4):1801–10. doi:10.1007/s00894-012-1750-3
  37. Allingham JS, Smith R, Rayment I. The structural basis of blebbistatin inhibition and specificity for myosin II. *Nat Struct Mol Biol* (2005) 12(4):378–9. doi:10.1038/nsmb908
  38. Wen H, Lu Y, Yao H, Buch S. Morphine induces expression of platelet-derived growth factor in human brain microvascular endothelial cells: implication for vascular permeability. *PLoS One* (2011) 6(6):e21707. doi:10.1371/journal.pone.0021707
  39. Duan M, Xing Y, Guo J, Chen H, Zhang R. Borneol increases blood-tumour barrier permeability by regulating the expression levels of tight junction-associated proteins. *Pharm Biol* (2016) 54:3009–18. doi:10.1080/13880209.2016.1199044
  40. Yang L, Kowalski JR, Zhan X, Thomas SM, Luscinskas FW. Endothelial cell cortactin phosphorylation by Src contributes to polymorphonuclear leukocyte transmigration in vitro. *Circ Res* (2006) 98(3):394–402. doi:10.1161/01.RES.0000201958.59020.1a
  41. Wenceslau CF, McCarthy CG, Webb RC. Formyl peptide receptor activation elicits endothelial cell contraction and vascular leakage. *Front Immunol* (2016) 7:297. doi:10.3389/fimmu.2016.00297
  42. Wiggins-Dohlvik K, Oakley RP, Han MS, Stagg HW, Alluri H, Shaji CA, et al. Tissue inhibitor of metalloproteinase-2 inhibits burn-induced derangements and hyperpermeability in microvascular endothelial cells. *Am J Surg* (2016) 211(1):197–205. doi:10.1016/j.amjsurg.2015.08.016
  43. Li Y, Hadden C, Cooper A, Ahmed A, Wu H, Lupashin VV, et al. Sepsis-induced elevation in plasma serotonin facilitates endothelial hyperpermeability. *Sci Rep* (2016) 6:22747. doi:10.1038/srep22747
  44. Allen CL, Bayraktutan U. Antioxidants attenuate hyperglycaemia-mediated brain endothelial cell dysfunction and blood-brain barrier hyperpermeability. *Diabetes Obes Metab* (2009) 11(5):480–90. doi:10.1111/j.1463-1326.2008.00987.x
  45. Fong LY, Ng CT, Zakaria ZA, Baharudin MT, Arifah AK, Hakim MN, et al. Asiaticoside inhibits TNF-alpha-induced endothelial hyperpermeability of human aortic endothelial cells. *Phytother Res* (2015) 29(10):1501–8. doi:10.1002/ptr.5404
  46. Yang M, Chen XM, Du XG, Cao FF, Vijaya Luxmi S, Shen Q. Continuous blood purification ameliorates endothelial hyperpermeability in SAP patients with MODS by regulating tight junction proteins via ROCK. *Int J Artif Organs* (2013) 36(10):700–9. doi:10.5301/ijao.5000216
  47. Zhu HQ, Wang XB, Han JX, Hu ZP, Wang Y, Zhou Q, et al. Myosin light chain kinase inhibitor attenuates atherosclerosis and permeability via reduced endothelial tight junction in rabbits. *Int J Cardiol* (2013) 168(5):5042–3. doi:10.1016/j.ijcard.2013.07.219
  48. Mizze MR, Nijland PG, van der Pol SM, Drexhage JA, van Het Hof B, Mebius R, et al. Astrocyte-derived retinoic acid: a novel regulator of blood-brain barrier function in multiple sclerosis. *Acta Neuropathol* (2014) 128(5):691–703. doi:10.1007/s00401-014-1335-6
  49. Thurston G, Suri C, Smith K, McClain J, Sato TN, Yancopoulos GD, et al. Leakage-resistant blood vessels in mice transgenically overexpressing angiopoietin-1. *Science* (1999) 286(5449):2511–4. doi:10.1126/science.286.5449.2511
  50. Kalliolias GD, Ivashkiv LB. TNF biology, pathogenic mechanisms and emerging therapeutic strategies. *Nat Rev Rheumatol* (2016) 12(1):49–62. doi:10.1038/nrrheum.2015.169
  51. Hu G, Minshall RD. Regulation of transendothelial permeability by Src kinase. *Microvasc Res* (2009) 77(1):21–5. doi:10.1016/j.mvr.2008.10.002
  52. Chen XL, Nam JO, Jean C, Lawson C, Walsh CT, Goka E, et al. VEGF-induced vascular permeability is mediated by FAK. *Dev Cell* (2012) 22(1):146–57. doi:10.1016/j.devcel.2011.11.002
  53. Mehta D, Malik AB. Signaling mechanisms regulating endothelial permeability. *Physiol Rev* (2006) 86(1):279–367. doi:10.1152/physrev.00012.2005
  54. Toda R, Kawazu K, Oyabu M, Miyazaki T, Kiuchi Y. Comparison of drug permeabilities across the blood-retinal barrier, blood-aqueous humor barrier, and blood-brain barrier. *J Pharm Sci* (2011) 100(9):3904–11. doi:10.1002/jps.22610
  55. Rochford KD, Cummins PM. Cytokine-mediated dysregulation of zonula occludens-1 properties in human brain microvascular endothelium. *Microvasc Res* (2015) 100:48–53. doi:10.1016/j.mvr.2015.04.010
  56. Kim LC, Song L, Haura EB. Src kinases as therapeutic targets for cancer. *Nat Rev Clin Oncol* (2009) 6(10):587–95. doi:10.1038/nrclinonc.2009.129
  57. van Vliet C, Bukczynska PE, Puryer MA, Sadek CM, Shields BJ, Tremblay ML, et al. Selective regulation of tumor necrosis factor-induced Erk signaling by Src family kinases and the T cell protein tyrosine phosphatase. *Nat Immunol* (2005) 6(3):253–60. doi:10.1038/ni1169
  58. Cheski BJ, Greger J, Cooch N, McNally C, McLarney S, Lam HS, et al. MNAR plays an important role in ERa activation of Src/MAPK and PI3K/Akt signaling pathways. *Steroids* (2008) 73(9–10):901–5. doi:10.1016/j.steroids.2007.12.028
  59. Cai H, Liu W, Xue Y, Shang X, Liu J, Li Z, et al. Roundabout 4 regulates blood-tumor barrier permeability through the modulation of ZO-1, Occludin, and Claudin-5 expression. *J Neuropathol Exp Neurol* (2015) 74(1):25–37. doi:10.1097/NEN.0000000000000146
  60. Li Z, Liu XB, Liu YH, Xue YX, Liu J, Teng H, et al. Low-dose endothelial monocyte-activating polypeptide-II increases blood-tumor barrier permeability by activating the RhoA/ROCK/PI3K signaling pathway. *J Mol Neurosci* (2016) 59(2):193–202. doi:10.1007/s12031-015-0668-5
  61. Suzuki T, Hara H. Role of flavonoids in intestinal tight junction regulation. *J Nutr Biochem* (2011) 22(5):401–8. doi:10.1016/j.jnutbio.2010.08.001
  62. Zheng CY, Song LL, Wen JK, Li LM, Guo ZW, Zhou PP, et al. Tongxinluo (TXL), a traditional Chinese medicinal compound, improves endothelial function after chronic hypoxia both in vivo and in vitro. *J Cardiovasc Pharmacol* (2015) 65(6):579–86. doi:10.1097/FJC.0000000000000226
  63. Wang L, Wang N, Tan HY, Zhang Y, Feng Y. Protective effect of a Chinese medicine formula He-Ying-Qing-Re formula on diabetic retinopathy. *J Ethnopharmacol* (2015) 169:295–304. doi:10.1016/j.jep.2015.04.031

**Conflict of Interest Statement:** The authors declare that the research was conducted in the absence of any commercial or financial relationships that could be construed as a potential conflict of interest.

Copyright © 2017 Zhang, Han, Zhao, Lv, Hu, Tan, Bi, Yu and Kou. This is an open-access article distributed under the terms of the Creative Commons Attribution License (CC BY). The use, distribution or reproduction in other forums is permitted, provided the original author(s) or licensor are credited and that the original publication in this journal is cited, in accordance with accepted academic practice. No use, distribution or reproduction is permitted which does not comply with these terms.